

BELLCOMM, INC.

1100 Seventeenth Street, N.W. Washington, D. C. 20036

SUBJECT: Spacecraft Shadowing and Thermal
Flux Computer Programs with Sample
Problems - Case 620

DATE: July 8, 1968

FROM: J. W. Powers

ABSTRACT

Two computer programs relating to spacecraft thermal analysis have been obtained from the Thermophysics Branch of Goddard Space Flight Center. These programs have been reviewed and adapted for Bellcomm computer use. Sample problems are described explaining the use of the programs. Possible modifications to increase the general utility of the programs are discussed.

One of these programs computes the surface areas of certain arbitrarily oriented elementary figures that are normal to a general solar vector. This program can also compute the total projected shadow cast upon any single figure by all other specified figures within certain limits.

The other program computes direct solar, planet-reflected solar, and planet-emitted infrared fluxes impinging on one surface of an arbitrarily located unit area in a planet orbit. The unit area may be in either a planet or inertial orientation and may be spinning.

(NASA-CR-96028) SPACECRAFT SHADOWING AND
THERMAL FLUX COMPUTER PROGRAMS WITH SAMPLE
PROBLEMS (Bellcomm, Inc.) 35 p

N79-72330

Unclas

00/18 11243

FF No. 602(A)	PROJECT NUMBER	(THRU)
	(PAGES)	(CODE)
	CP-96028	
	(NASA CR OR TMX OR AD NUMBER)	



BELLCOMM, INC.

1100 Seventeenth Street, N.W. Washington, D. C. 20036

SUBJECT: Spacecraft Shadowing and Thermal
Flux Computer Programs with Sample
Problems - Case 620

DATE: July 8, 1968

FROM: J. W. Powers

MEMORANDUM FOR FILE

INTRODUCTION

An adequate and efficient spacecraft thermal design requires detailed knowledge in many disciplines. These required disciplines range from materials properties to projective geometry and orbital mechanics. The accurate determination of spacecraft incident direct and secondary thermal flux considering a general orientation and self-shadowing is an effort of major proportions.

Two computer programs which facilitate determination of spacecraft incident thermal flux have been developed by the Thermophysics Branch of Goddard Space Flight Center. These two computer programs have been adapted for Bellcomm computer use. The intrinsic capabilities and limitations of both programs are described. Sample problems illustrating the use of both programs are presented.

SPACECRAFT SHADOWING PROGRAM

Capabilities

- . This program computes the surface areas normal to a general solar vector for certain arbitrarily oriented geometric figures. In a system of arbitrarily oriented nonspinning figures, the program also computes the total projected shadow area cast on any figure by all the other figures within certain limits.
- . In any spacecraft configuration a maximum of eight surfaces may shade any other surface.
- . A spacecraft may be defined by a maximum of 50 figures with combinations of the following geometries:
 - . Convex planes (maximum of 10 vertices)
 - . Elliptical or circular discs (maximum of 10)
 - . Cones and conical frustums (maximum of 12)
 - . Circular cylinders (maximum of 12)
 - . Spheres (maximum of 12)

Limitations

- . Skew planes are not easily incorporated since coordinates of vertices must be determined as input. (Appendix I develops the analysis for skew plane geometry)
- . Input solar vector angles must be related to general orbital parameters if a particular case is to be investigated. (Appendix II develops this analysis)
- . If more than 40 intersection points occur on any figure, the shaded area cannot be computed.
- . Surfaces other than those listed can not be considered or must be approximated by combinations of listed figures.

Discussion

The shadowing program is based upon the analysis in Reference 1. An arbitrary spacecraft coordinate system X,Y,Z is defined and the solar vector is related to the spacecraft by the angles ν and λ . The X,Y,Z system is rotated through an angle Δ thus positioning the X'-axis coincident with the solar vector. The new coordinate system's Y'-Z' plane is normal to the solar vector. The resultant transformation matrix* (equation 10, Reference 1) is shown below. Figure I shows the angles.

$$\begin{pmatrix} X' \\ Y' \\ Z' \end{pmatrix} = \begin{bmatrix} \cos \nu \sin \lambda & \sin \nu \sin \lambda & \cos \lambda \\ 0 & \frac{-\cos \lambda}{\sin \Delta} & \frac{\sin \nu \sin \lambda}{\sin \Delta} \\ \sin \Delta & \frac{-\sin \nu \cos \nu \sin^2 \lambda}{\sin \Delta} & \frac{-\cos \nu \sin \lambda \cos \lambda}{\sin \Delta} \end{bmatrix} \begin{pmatrix} X \\ Y \\ Z \end{pmatrix}, \quad (1)$$

*A much simpler transformation is obtained by first performing a positive rotation ν about the Z-axis followed by a negative rotation $(90-\lambda)$ about the Y-axis. These two rotations yield the transformation matrix.

$$\begin{pmatrix} X^* \\ Y^* \\ Z^* \end{pmatrix} = \begin{bmatrix} \cos \nu \sin \lambda & \sin \nu \sin \lambda & \cos \lambda \\ -\sin \nu & \cos \nu & 0 \\ -\cos \nu \cos \lambda & -\sin \nu \cos \lambda & \sin \lambda \end{bmatrix} \begin{pmatrix} X \\ Y \\ Z \end{pmatrix}, \quad (2)$$

The difference between transformation matrices (1) and (2) is the angular position of the Y*-Z* axes relative to the Y'-Z' axes. By considering either the Y' and Y* or Z' and Z* axes, the angle

between these respective pairs of axes is seen to be $\cos^{-1} \left(-\frac{\cos \nu \cos \lambda}{\sin \Delta} \right)$.

Figure 1 shows the solar vector angles, where $s_{\Delta} = \sqrt{c_{\lambda}^2 + s_{\lambda}^2 v s^2}$ *

Transformed coordinates of a plane surface are computed by use of (1). The area in the Y'-Z' plane is the area normal to the solar vector. This area is determined by dividing the polygon into triangles having a common vertex at the polygon centroid and summing the areas of all resultant triangles.

The area of one surface shaded by another is determined in the Y'-Z' plane by consideration of interior vertices and vertices formed by intersections of straight line segments of different surfaces. At a vertex formed by the intersection of two different projected perimeters in the Y'-Z' plane, the greater X' coordinate determines which surface shades the other. The net shaded area of several mutually overlapping surfaces is determined by an elegant application of combinatorial analysis.

Cylinders and cones are approximated by 32-sided polygons and another coordinate system is utilized for their axes of symmetry. Projected areas of cylinders and cones computed by the program include end areas.

Shadowing Program Sample Problem

To illustrate program use, a simple example is used which consists of a cylindrical body, two transverse rectangular panels representing solar arrays, and a transverse conical frustum module. The model with required coordinates is shown in Figure 1. For the convenience of working with all positive coordinates, the cylinder axis is taken at the line (50,50,Z) in the first octant.

For this problem the solar angle v is fixed at 45° and the other solar angle, λ is varied between 15° and 75° . The projected unshaded area normal to the solar vector as a function of λ for each of the components is shown in Figure 2. Because of the solar vector angles selected, plane II and conical frustum IV receive no shading. Cylinder III and plane I are both shaded by one or more of the other surfaces. Table I shows the shaded areas and shading figures as functions of the selected solar angles. Quantities in parenthesis are percentages of total projected areas which are shaded.

To allow the computer to distinguish positively between figures, finite spacing between model elements is required. In the sample problem a spacing of one unit is used between the three elements which are attached to the cylinder.

*The notation $s()$ and $c()$ is used for $\sin()$ and $\cos()$

TABLE I

SOLAR ANGLES	PROJECTED AREA SHADED, FT ² (% SHADED AREA)			
$\nu = 45^\circ$	Shading Figure(s)		Shading Figure(s)	
λ				
	PLANE I		CYLINDER III	
15	III, IV	14.8 (11.5)	II, IV	63.6 (8.0)
30	III, IV	122.6 (49.3)	II, IV	86.3 (7.5)
45	III, IV	147.9 (42.0)	II, IV	105.0 (7.3)
60	III	47.9 (11.1)	II, IV	118.0 (7.3)
75	III	53.4 (11.1)	II, IV	124.5 (7.4)

Appendix III shows the required computer input format for the shadowing program and the coding sheet for $\lambda = 15^\circ$ and 30° in the sample problem.

SOLAR FLUX PROGRAM

Capabilities

- Determines incident direct solar radiation, planet reflected solar radiation (albedo), and planet emitted infrared radiation on one surface of an arbitrarily oriented unit area in a general orbit about a planet.
- Unit area surface may have any inertial or planet orientation and may be spinning about any axis at a high rate.
- Computes orbital angles, times and radius vectors for entry and exit from shadow zone.
- Any planet may be input with appropriate constants (radius, maximum and minimum temperatures, albedo, solar constant, and gravity constant). Constants for earth and moon are programmed.
- Planet may have either a constant temperature (earth model) or a cosine varying temperature with a maximum at subsolar point and minimum at terminator and shadowed hemisphere (moon model).

- . Computes radius vector from occupied focus to orbital position and time of flight from perigee.
- . A blockage factor* table (unshaded projected area/total projected area) as a function of the two solar angles** may be determined from the shadowing program. This table is input into the flux program. The appropriate blockage factor for a particular solar orientation is determined by double linear interpolation and is utilized in the computations.

Limitations

- . Only planar geometry can be handled directly. Other figures must be approximated by planes.
- . The umbra shadow is considered as a circular cylinder rather than a cone. Since the conical shadow included angle is approximately 0.5° , negligible error is introduced for earth orbits up to synchronous altitudes.
- . Penumbra effects are not considered.
- . Solar vector angles must be related to general orbital parameters if a particular case is to be investigated. (Appendix II develops the analysis)
- . Program spin capability is only directly applicable to panel spin rates much greater than the orbital angular velocity. For low spin rates (\sim orbital angular velocity), the input orbital angular and panel rotational angular increments may be selected to yield the required data. This procedure, which is discussed later, requires excessive output generation and tedious manual data review.

Discussion

The solar flux program is developed from the analysis in Reference 2, which considers only inertial panel orientations.

Direct solar flux incident on the panel is determined from the dot product of the solar and panel unit normal vectors. To determine planet emitted IR flux, the analysis assumes that the earth is a 450°R diffusely emitting spherical black body.

*GSFC terminology, in reality an "unblocked" factor.

** ν and λ from page 2.

The visible spherical segment of the earth "seen" by the panel is divided into a desired number of nodes and the program integrates the incident IR flux from all nodes (Equation 14, Reference 2). Accuracy may be varied in the program by an appropriate choice of the number nodes. The albedo flux calculation is performed in a manner similar to the earth IR flux determination. The geometry factor for albedo radiation is equal to the earth emitted IR factor with inclusion of the cosine of the angle between the local earth normal and solar vector. The albedo view factor must also consider only unshadowed portions of the earth's surface. For planet reflected radiation, an approximate mean albedo is used (0.35 and 0.07 are the respective programmed earth and moon values).

Program input requires angular specification of three vectors; solar, spin axis, and surface normal at perigee conditions. The coordinate system used in the program for the surface normal is different from that shown in Reference 2. The three required vectors and their associated coordinate systems are shown in Figure 3. The X,Y,Z coordinate system is referred to orbital conditions and is fixed at the perigee. The X-Y plane is in the orbital plane and the positive X direction is along the line from the planet to the perigee. Direction of panel movement in the orbit fixes the positive Y-direction. The sun pointing solar vector is specified relative to the X,Y,Z, orbital system with angles ν and λ . This solar vector specification is different from that of the shadowing program where the angles are measured from a spacecraft coordinate system.

The spin axis coordinate system XTP, YTP, ZTP is also specified relative to the X,Y,Z system. ZTP is the spin axis and is located with two angles μ_Z and δ_Z . The projection of the XTP-axis in the X-Y plane is specified by the angle δ_X . If μ_Z is 90° or 270° , an angle μ_X must be used to fix the rotational position of the XTP-YTP plane from the Z axis.

The panel normal axis is located relative to the spin axis coordinate system rather than the orbital coordinate system. Angles β and γ specify the panel normal axis relative to spin axis coordinate system. For a nonspinning panel the angles specifying the spin coordinate system and the number of spin axis increments are input as zero. With a nonspinning configuration the coordinates β and γ are referred directly to the orbital plane coordinate system.

Thermal Flux Sample Problem I

To illustrate use of the thermal flux program, the unit area plane is considered in a circular earth orbit with

an inertial orientation normal to the sun line. To assist in geometric visualization, the sun is considered in the orbital plane, thus yielding the minimum sunlight time for a given orbit. Increasing the angle between the orbital plane and sun line causes the in-shadow travel time to decrease. Because of the plane's inertial orientation, the sun facing surface receives a direct solar flux of 440 Btu/hr-ft^2 for the total nonshadowed travel time. The plane surface away from the sun of course receives no direct solar flux.

Earth reflected solar radiation (albedo) and earth emitted IR are functions of orbital altitude (both diminish with increasing altitude) and surface orientation. Albedo flux, like solar flux, is zero in the shadow zone. For a 230 NM circular orbit altitude with the sun in the orbital plane ($\nu = 0^\circ$, $\lambda = 90^\circ$), the albedo and earth IR flux were computed for both the light ($\beta = 0^\circ$, $\gamma = 90^\circ$) and dark ($\beta = 180^\circ$, $\gamma = 90^\circ$) panel surfaces. Figure 4 shows these fluxes as a function of in-orbit angular position from the subsolar point. Maximum albedo and earth emitted IR both occur on the dark panel side at the orbital noon position. At this point, the panel is normal to the local vertical and the maximum panel to earth view factor exists. In the shadow zone, maximum earth emitted IR occurs on the light surface when it is 180° away from the orbital noon position. The earth emitted IR curves for the dark and light panel sides are seen to be identical except for 180° of angular displacement.

As a consequence of the simple earth model used, earth emitted IR is independent of both the sun's position and the particular area of the earth viewed by the panel. The magnitude of earth emitted IR is dependent only upon panel orientation relative to earth and altitude. With an inertial orientation, the view factor changes as a function of in-orbit position. With a planet orientation the earth emitted IR view factor for a plane remains constant in a circular orbit.

If the "seen" portion of the earth's surface does not include a shadowed area, the albedo flux on the inertially oriented panel is proportional to the cosine of the in-orbit angle from the earth-sun line. Maximum albedo flux occurs on the panel dark surface at the orbital noon position.

Thermal Flux Sample Problem II

Consider a unit area surface in an earth oriented 230 NM circular orbit with the panel normal maintained in the local horizontal direction. This sample problem determines the

three thermal fluxes incident upon one surface of a nonspinning unit area.

For visualization simplicity the solar vector is again considered in the orbital plane. Surface orientation is selected so that normal direct solar impingement occurs after 270° of orbital travel from orbital noon (β and $\gamma = 90^\circ$). With this orientation the specified surface receives no direct solar radiation in traveling from the subsolar point to just before emergence from the shadow zone (249.6° of travel). Upon emergence from the shadow zone, the surface receives increasing solar flux to a maximum at 270° of angular travel. With this panel orientation the flux impingement experienced is a cosine function with zero magnitude at the subsolar point. Figure 5 shows the three thermal fluxes for an earth oriented plane surface as a function of angular position.*

Constant orbital altitude and surface orientation yield an earth emitted IR panel-earth view factor which is independent of in-orbit angular position. This orientation results in an incident constant earth emitted IR flux of 20.2 Btu/hr-ft^2 on the panel surface.

For albedo flux, the panel-earth view factor will change with panel angular position in the orbit. This changing view factor is a consequence of the surface "seeing" shadowed and unshadowed portions of the earth's surface. Maximum albedo flux in the selected planet orientation occurs upon passage through the earth-sun line where the cosine effect is absent. Albedo flux is zero during orbital travel in the shadow zone.

Appendix IV shows the required computer input format for the thermal flux program.

Cylinder and Conical Approximations and Low Spin Rates

If a cylindrical or conical surface is to be considered in a particular orbit with this program, it must be approximated by a polygonal cylinder or a n-sided right rectangular pyramid. Use of the program's spin capability allows a polygon approximation to be input very simply. The figure's longitudinal axis is input as the spin axis. The desired number of angular increments around the spin axis (number of polygon sides) and the angular specification of one of the figure's sides are also input. One 360° panel rotation is performed by the program at each selected orbital angular increment. The three thermal fluxes

*For the other panel surface simply consider the angular position to be measured from the right rather than left in Fig. 5

on one side of the spinning surface are averaged both at each orbital angular increment and over the entire orbit, considering shadowing. The program uses 100 spin increments for the solar flux with any spin axis angular increment input <100 .

To evaluate the effect of number of cylinder polygon sides several cases were considered with both 8 and 100 surfaces. A nonrolling cylinder was considered in a 230 NM circular orbit with both gravity-gradient (GG) and perpendicular to orbital plane (POP) orientations. For angles between the sun line and orbital plane of 0° and 53° , the average direct solar flux incident upon the cylinder lateral surface was computed. For 8 and 100 faces, the direct solar flux acting on each face was determined at each 15° of orbital travel and averaged over the orbit. The overall average flux was determined from the mean of the fluxes incident upon the respective cylinder sides. The maximum error in direct solar average flux induced by considering 8 sides in comparison with 100 sides for the cases listed is -5.2% and occurs with a GG orientation and a 53° sun angle. For the other cases the resultant error is $<1\%$.

To evaluate incident flux on a panel with a low spin rate, a selective procedure must be utilized. If S_α and S_κ are the desired orbital and panel spin rates, $S_\kappa = CS_\alpha$, where C is an integer or the reciprocal of an integer. If m is the number of orbital angular increments, the orbital angular increment is $\Delta\alpha = 360/m$. The number of spin angle angular increments is $n = 360/C\Delta\alpha$. The program requires that input variables m and n be specified as even integers, thus restricting the possible value of C .

Input specification of the panel's normal and spin axes at perigee are required. For circular orbits the orbital noon is the most convenient reference position. The program is designed so that spin increments at each orbital increment commence from the initial surface orientation. The output format will yield n sets of thermal flux data for each orbital angle position. For the k^{th} angular increment in a particular orbit, the k^{th} row of thermal data is utilized. By appropriate data selection the incident thermal flux on a panel as a function of orbital position is thus determined. Only $1/n$ of the output is utilized with this procedure.

There is current interest in the AAP Program in the POP and GG spacecraft orientations with a controlled spacecraft roll rate equal to the orbital angular rate. This orientation for the POP mode is simply input as an inertial case* with the spin axis coincident with the Z-axis. The procedure for obtaining both the flux on the individual polygon sides and the average flux is as described above.

The GG orientation with a roll rate equal to the orbital rate is a more involved problem and can be handled in a manner analogous to the low spin rate panel. The cylinder axis at the perigee is input as the spin axis $\delta_z = 0$, $\mu_z = 90$, $\delta_x = 0$ and $\mu_x = 180$). The number of orbital angular increments is selected equal to the number of polygon sides, N , desired and an equal number of spin angle increments are input. The surface normals for each side are input ($\beta = 0$, $\gamma = 90$), ($\beta = 360/N$, $\gamma = 90$), ..., ($\beta = (N-1)360/N$, $\gamma = 90^\circ$). The resultant output for each orbital angular increment for each set of corresponding normal angles (β, γ) will contain N rows of thermal data corresponding to the N polygon sides. The only data from each run which is appropriate for this problem, however, is for the condition $\alpha = \beta$. For any set of data $\alpha = \beta$, the k^{th} row ($N \geq k$) always corresponds to the k^{th} polygon side. Averaging the respective thermal fluxes incident upon corresponding polygon sides yields the desired data. The program has been edited to eliminate extraneous data computation and printout for this type of problem. For normal problems the program is unchanged.

Table II shows thermal data for different orbital orientations, sun angles, and with and without roll for the lateral surface of a 8-sided polygonal cylinder. Symmetry of the direct solar and albedo flux variation around the polygon perimeter is apparent. The polygon faces are numbered in a counter-clockwise direction with the number one face receiving most direct solar impingement at the noon position. For the GG orientation with no roll ($\beta = 0$), sides 1 and 5 are normal to the orbital plane's normal and thus receive no direct solar flux.

Thermal Flux Sample Problem III

The albedo and earth emitted IR flux on an AAP CM-SM module in an inertial orientation are of current interest. The CM cone is approximated by a 8-sided right rectangular pyramid with its axis and apex pointed at the sun. A 8-sided polygonal

*Low nodal regression rates result in this model being approximately correct for a single orbital period.

cylinder having the same axis and extending from the pyramid's base is used for the SM model. The program was used to determine the average flux on the cone and cylinder lateral surfaces and the cylinder end away from the sun. The effect of any shading by solar arrays or the SPS nozzle was not included

Sun angles of 51° and 73° were considered with the vehicle in a 230 NM circular earth orbit. The program coding form for this problem is shown in Appendix IV. The average flux incident upon the total surface was determined from

$$\bar{Q} = \frac{2Q_{cy}L/R + Q_{co}/\sin\phi + Q_e}{2L/R + 1/\sin\phi + 1}$$

where $Q_{cy,co,e}$ are the respective average fluxes impinging on the cylinder, cone, and cylinder end. L and R are the cylinder length and radius. ϕ is the cone half angle. Figure 6 shows the albedo and IR average fluxes as functions of the angle measured from the orbital noon position. The numerical calculations show that the averaged IR flux incident upon any simple* spacecraft geometry is essentially independent of orientation and dependent only upon altitude. The reason for the different averaged IR fluxes for the GG and POP orientations shown in Table II is that the cylinder ends were not included. Inclusion of both ends results in an averaged IR flux of approximately 23 Btu/hr-ft² for both orbital orientations.

Appendix V discusses thermal fluxes on a spherical surface and a sphere approximation.

ACKNOWLEDGMENT

Mr. J. T. Skladany, Aerospace Engineer at the Thermophysics Branch, NASA Goddard Space Flight Center developed and provided the two described programs. He also gave many hours of advice pertaining to their use and spacecraft thermal problems in general. His assistance is greatly appreciated. Mr. C. O. Guffee and Mrs. Barbara Lab were responsible for adapting the programs for use on the Bellcomm computer.

J. W. Powers
J. W. Powers

1022-JWP-bjw

Attachments

Table II
Appendices I-V
Figures 1-7
References

*Cylinders, cones and polyhedra with certain combinations that are figures of revolution without direct shadowing.

TABLE II

ORBIT AVERAGED THERMAL FLUX INCIDENT UPON POLYGONAL CYLINDER SIDES

ORIENTATION	B°	AVG Thermal Flux	POLYGONAL SIDE NUMBER								
			1	2	3	4	5	6	7	8	AVG*
GG W/ROLL	0	Q _S	165.0	116.7	27.5	0	0	0	27.5	116.7	57.7
	0	Q _A	14.4	14.2	13.3	12.8	12.6	12.8	13.3	14.1	13.2
	0	Q _{IR}	↔	↔	↔	↔	20.2	↔	↔	↔	20.2
GG, W/NO ROLL	0	Q _S	0	66.4	93.9	66.4	0	66.4	93.9	66.4	59.8
	0	Q _A	↔	↔	↔	↔	13.8	↔	↔	↔	13.8
	0	Q _{IR}	↔	↔	↔	↔	20.2	↔	↔	↔	20.2
GG W/ROLL	53	Q _S	203.4	165.4	76.7	21.6	0	21.6	76.7	165.4	89.9
	53	Q _A	9.7	9.3	8.3	7.2	6.8	7.2	8.3	9.3	8.2
	53	Q _{IR}	↔	↔	↔	↔	20.2	↔	↔	↔	20.2
GG W/NO ROLL	53	Q _S	244.8	173.1	66.2	0	0	0	66.2	173.1	90.1
	53	Q _A	9.9	9.4	8.4	7.3	6.9	7.3	8.3	9.3	8.4
	53	Q _{IR}	↔	↔	↔	↔	20.2	↔	↔	↔	20.2
POP W/ROLL	0	Q _S	269.9	190.8	0	0	0	0	0	190.8	85.9
	0	Q _A	2.2	5.9	16.0	27.7	33.0	27.7	16.0	5.9	16.6
	0	Q _{IR}	↔	↔	↔	↔	24.2	↔	↔	↔	24.2
POP W/ROLL	53	Q _S	184.5	130.4	0	0	0	0	0	130.4	58.7
	53	Q _A	1.4	3.6	9.7	16.7	19.9	16.7	9.7	3.6	10.0
	53	Q _{IR}	↔	↔	↔	↔	24.2	↔	↔	↔	24.2

B, Angle Between Sun Line and Orbital Plane, Deg

Q_S, Direct Solar Flux, Btu/hr-ft²Q_A, Albedo Flux, Btu/hr-ft²Q_{IR}, Earth Radiated Flux, Btu/hr-ft²

* AVG. Values in some cases are based on more than 8 sides

230 NM Circular orbit

APPENDIX I

SKEW PANEL ANALYSIS

Consider a hinged panel system with two-degree of freedom rotational capability. Let the panel coordinates be X, Y, Z relative to the hinge coordinate system and the coordinates of the hinge be X_h, Y_h, Z_h in the spacecraft coordinate system X', Y', Z' . Let the respective axes of the X, Y, Z and X', Y', Z' coordinate systems be parallel and have the same positive directions.

A positive rotation θ about the Z -axis followed by a positive rotation ϕ about the now rotated Y -axis may be written in terms of a transformation matrix. This matrix, which relates the original panel coordinate system to the rotated coordinate system X_o, Y_o, Z_o is

$$\begin{pmatrix} X_o \\ Y_o \\ Z_o \end{pmatrix} = \begin{bmatrix} c\theta c\phi & s\theta c\phi & -s\phi \\ -s\theta & c\theta & 0 \\ c\theta s\phi & s\theta s\phi & c\phi \end{bmatrix} \begin{pmatrix} X \\ Y \\ Z \end{pmatrix}$$

The rotated panel system is related to the spacecraft coordinate system by the coordinates of the hinge axis

$$X' = X_h + c\theta c\phi X + s\theta c\phi Y - s\phi Z$$

$$Y' = Y_h - s\theta X + c\theta Y$$

$$Z' = Z_h + c\theta s\phi X + s\theta s\phi Y + c\phi Z$$

These coordinates may now be used in (1). This transformation allows a skewed panel to be considered if the before rotation vertex coordinates and rotational angle(s) are known.

Judicious selection of the spacecraft axis relative to the hinge axis can reduce two of the three hinge coordinates to zero and thus reduce computation time.

APPENDIX II

DETERMINATION OF PROGRAM SOLAR VECTOR ANGLES IN TERMS OF GENERAL ORBITAL PARAMETERS

An orbital coordinate system is defined with the X-Y plane in the orbital plane and the X-direction pointing toward the perigee. The Y-direction coincides with the radius vector after 90° of angular travel. The matrix which transforms the orbital coordinate system X,Y,Z to an equatorial coordinate system X',Y',Z' is given in Reference (3)*

$$\begin{pmatrix} X' \\ Y' \\ Z' \end{pmatrix} = \begin{bmatrix} c\Omega c\omega & -c\Omega s\omega & s\Omega si \\ -s\Omega ci s\omega & -s\Omega ci c\omega & \\ s\Omega c\omega & -s\Omega s\omega & -c\Omega si \\ +c\Omega ci s\omega & +c\Omega ci c\omega & \\ sis\omega & sic\omega & ci \end{bmatrix} \begin{pmatrix} X \\ Y \\ Z \end{pmatrix}, \quad (\text{II-1})$$

where

i = inclination angle between orbital and equatorial planes

ω = argument of perigee

Ω = longitude of ascending node

The equatorial coordinate system can be transformed into an inertial system X'', Y'', Z'' by a suitable rotation. Consider the X'-axis coincident with the vernal equinox and rotate the equatorial coordinate system a positive angle e about the X' axis (e is the fixed angle between the equatorial and ecliptic planes). After this transformation the Y''-axis is pointing in the direction of winter solstice.

*The minus sign in the a₂₁ term of the corresponding equation in Reference (3) is incorrect and should be positive as shown above. Verification of the matrix may be obtained by performing negative rotations ω, i, and Ω about the Z, X, and Z axes.

The transformation matrix of the orbital coordinate system to the inertial coordinate system is

$$\begin{pmatrix} X'' \\ Y'' \\ Z'' \end{pmatrix} = \begin{bmatrix} a_{11} & a_{12} & a_{13} \\ \hline \text{ces}\Omega\text{c}\omega & -\text{ces}\Omega\text{s}\omega & -\text{cec}\Omega\text{s}i \\ +\text{cec}\Omega\text{c}i\text{s}\omega & +\text{cec}\Omega\text{c}i\text{c}\omega & +\text{sec}i \\ +\text{ses}i\text{s}\omega & +\text{ses}i\text{c}\omega & +\text{sec}i \\ \hline -\text{ses}\Omega\text{c}\omega & \text{ses}\Omega\text{s}\omega & \text{sec}\Omega\text{s}i \\ -\text{sec}\Omega\text{c}i\text{s}\omega & -\text{sec}\Omega\text{c}i\text{c}\omega & \\ +\text{ces}i\text{s}\omega & +\text{ces}i\text{c}\omega & +\text{cec}i \end{bmatrix} \begin{pmatrix} X \\ Y \\ Z \end{pmatrix}, \quad (\text{II-2})$$

The a_{11} , a_{12} and a_{13} terms are equal to the corresponding terms of (II-1).

If α is the angle between the unit solar vector and vernal equinox, the unit solar vector is $\bar{S}_0 = c\bar{i}'' + s\alpha\bar{j}''$ where \bar{i}'' and \bar{j}'' are ecliptic plane unit vectors in the X'' and Y'' directions. The vector dot product of \bar{S}_0 and the unit normal to the orbital plane is

$$\bar{S}_0 \cdot \bar{k} = a_{13}c\alpha + a_{23}s\alpha = c(90 + B)$$

where \bar{k} is the unit vector in the Z -direction whose components are obtained from the transpose of (II-2). B is the angle between the solar vector and orbital plane. After simplification

$$sB = s\alpha(\text{cec}\Omega\text{s}i - \text{sec}i) - c\alpha\Omega\text{s}i, \quad (\text{II-3})$$

This equation is given without proof with slightly different notation in Reference (4).

If Δ is the angle between the spacecraft X -axis and the solar vector

$$c\Delta = s\lambda c\nu \quad (\text{II-4})$$

where λ and ν are the solar vector angles used in the program. Since the X - Y plane is the orbital plane

$$\lambda + B = 90^\circ, \quad (\text{II-5})$$

The equation of the unit vector along the spacecraft X-axis is determined from the transpose of (II-2)

$$\bar{i} = a_{11}\bar{i}'' + a_{21}\bar{j}'' + a_{31}\bar{k}''$$

Taking the dot product of the unit vector \bar{i} and the unit solar vector \bar{S}_o .

$$c\Delta = \bar{i} \cdot \bar{S}_o = a_{11}c\alpha + a_{21}s\alpha$$

$$= c\alpha(c\Omega c\omega - s\Omega c i s\omega)$$

$$+ s\alpha[ce(s\Omega c\omega + c\Omega c i s\omega) + s e s i s\omega]$$

For a specific set of orbital parameters, $c\Delta$ and sB can be calculated.* The solar vector angles λ and v may then be determined from (II-5) and (II-4). This solution will be for perigee conditions. The flux program determines other angular positions from the input data. LK, an orbital increment variable, can be selected to give the desired in-orbit locations. In the shadow program, angular positions for other than perigee conditions must consider another angle. If f is the spacecraft in-orbit angular position measured from the perigee position, the column vector (X,Y,Z) in (II-2) is replaced by (rcf, rsf, Z). r is the radius vector to the orbital position determined by the angle f (true anomaly).

This analysis can be further extended to include the variables of time of day and time of year of launch.

*Consideration must be given to double valued trigonometric functions.

APPENDIX III

SHADING PROGRAM

INPUT DEFINITIONS

Card 1 TITLE

Card 2 Number of Fig.: Number of shaded Fig.:
output form (IWR) Format (3I6)

IWR = 0, full printout of (XYZ) and
(X'Y'Z') coordinates

IWR = -1, no printout of prime coordinates

IWR = 1, no printout of any coordinates

Card 3 Surface Geometry Data

Planes

Card 1 PØLYGN NAME Format (2A6)

Card 2 Number of vertices Format (I6)

Card 3 to N XYZ coordinates of all vertices
in either clockwise or counter-
clock wise order Format (6F12.2)

Cylinders

Card 1 CYLIND NAME Format (2A6)

Card 2 XYZ coordinates of centers
of upper and lower bases Format (6F12.2)

Card 3 Radius Format (F12.2)

Cones

Card 1 CØNE NAME Format (2A6)

Card 2 XYZ coordinates of centers of
upper and lower bases Format (6F12.2)

Card 3 Radii of upper and lower
bases Format (2F12.2)

Spheres

Card 1	SPHERE NAME	Format (2A6)
Card 2	XYZ coordinates of center: Radius	Format (4F12.2)

Disks

Card 1	DISK NAME	Format (2A6)
Card 2 and 3	XYZ coordinates of center: coordinates of major axis: coordinates of minor axis	Format (6F12.2)

If shading data is not desired for all surfaces
(first two numbers on second card are not equal), read in
names of surfaces whose shading is desired; otherwise omit
these cards

Format (12A6)

Last Card	Solar angles $\nu:\lambda$ Solar vector is <u>from</u> X,Y,Z coordinate system <u>to</u> sun	Format (2F12.2)
-----------	--	-----------------

For Other Solar Angles

Card 1	TITLE
Card 2	0 : number of shaded Fig: IWR
Card 3	Names of shaded surfaces if shading of all surfaces is not desired
Card 3 or 4	New solar angles $\nu:\lambda$

The included coding form gives input data format
for the sample problem.

BELLCO M, INC

CODING FORM

Programmer J.W. Powers
 Problem Shadowing
 Date Program

Page 1 of 2
 Identification 73 80

APPENDIX III

1	6	8	16	20	25	30	35	40	45	50	55	60	65	70
NAME														
4														
POLYG														
NONE														
4														
50.0														
50.0														
POLYG														
TWO														
4														
50.0														
50.0														
CYLIND														
THREE														
50.0														
11.0														
CONE														
FOUR														
62.0														
6.0														
45.0														
NAME														
0														
45.0														

FORTRAN COLUMNS: 1 C for comment 2 Statement number 6 Continuation 8 Comments 16 Statement
 MAP COLUMNS: 1 * for comment 2 Label 8 Operation 16 Variable field 36 Comments

APPENDIX IV

THERMAL FLUX PROGRAM

Input Definitions

Card 1

- NPLN - Planet No.; 0(earth); 1(moon); 2(any other)
NNØR - Number of surfaces to be evaluated requiring same information from card 1
LK - Angular increments in orbital plane (even number >0)
FKP - Perigee altitude (statute miles)
E - Orbit eccentricity ($0 \leq E < 1$)

If NPLN = 2, the following planet constants must be input. Quantities in parenthesis are programed constants for earth and moon.

- FLKRE - Radius (statute miles) (3960,1086)
TMAX - Maximum temperature ($^{\circ}\text{R}$) (450,673)
TMIN - Minimum temperature ($^{\circ}\text{R}$) (450,222)
SMA - Albedo (0.35,0.07)
SKS - Solar constant (Btu/hr-ft^2) (440,440)
CØN - Gravitational constant
(ft^3/sec^2) (1.408×10^{16} , 1.731×10^{14})

Card 2

- KD - No. of increments around spin axis (even no. >0). For no spin use 0
KDK - No. of increments (latitude) used in earth cap numerical integration (16 used in sample problems)
MK - No. of increments (longitude) used in earth cap numerical integration (32 used in sample problems)
IBLK - Blockage table; 0(no blockage); 1(blockage table must be input), See card 3
NEØ - Surface orientation; 0(inertial); 1(planet)

- XNU - Angle between X-axis and solar vector's projection in X-Y plane ($0 \leq XNU \leq 360$)
- XLAM - Angle between Z-axis and solar vector ($0 \leq XLAM \leq 180$)
- BETA - Angle between XTP-axis and surface normal's projection in XTP-YTP plane ($0 \leq BETA \leq 360^\circ$)
- GAM - Angle between ZTP-axis and surface normal ($0 \leq GAM \leq 180$)
- DELTA - Angle between X-axis and ZTP-axis's projection in X-Y plane. ($0 \leq DELTA \leq 360$)
- AMU - Angle between Z-axis and ZTP-axis ($0 \leq AMU \leq 180$)
- DELX - Angle between X-axis and ZTP-axis's projection in X-Y plane ($0 \leq DELX \leq 360$)
- AMUX - Angle between Z-axis and XTP-axis ($0 \leq AMUX \leq 180^\circ$)
input only if $AMU = 90^\circ$ or 270°

Card 3, etc.

Blockage Table, input only if IBLK = 1

NNU - No. ZNU angles input

NLAM - No. ZLAM angles input

ZNU - Angle between XTP-axis and solar vector's projection on XTP-YTP plane ($0 \leq ZNU \leq 360$)

ZLAM - Angle between ZTP-axis and solar vector ($0 \leq ZLAM \leq 180$)

BL(I,J) - Blockage factors, $I = 1$, NNU and $J = 1$, NLAM

The included coding forms show the input data format for a general problem and thermal flux problem III.

Programmer	<u>J. W. Powers</u>
Problem	<u>Flux Program</u>
Date	

Page 1 of 1
Identification 73 80

[illegible]

FORTRAN COLUMNS:						
1	C	for comment	2	Statement number	6	Continuation
8						
16						
					8	Comments
					16	Statement
MAP COLUMNS:						
1	*	for comment	2	Label		
8					8	Operation
16					16	Variable field
36						Comments

Page 1 of 1
Identification 73 80

Programmer	J.W. Powers
Problem	Cone-Cylinder
Date	Flux Program

APPENDIX IV

	6	8	16	20	25	30	35	40	45	50	55	60	65	70
0.612	265.0	0.0												
81632	0	0.0	17.0	0.0	90.0	90.0	0.0	0.0	17.0	0.0				
						57.0							B=73° CONE CYL	
						180.0							CONE END	
			33.0			90.0			39.0				B=51° CONE CYL	
						57.0							CONE END	
						180.0								

[illegible]

APPENDIX V

THERMAL FLUXES INCIDENT UPON A SPHERE AND A SPHERE APPROXIMATION

Approximation techniques for cylindrical and conical surfaces used with the Thermal Flux Program were discussed previously. This appendix considers the three thermal fluxes incident upon a sphere in a circular earth orbit.

From elementary considerations the direct solar flux, Q_S , at 1 A.U. is

$$Q_S = \pi r^2 S$$

With a more involved analysis, the earth emitted IR radiation, Q_{IR} , from Reference 5 is

$$Q_{IR} = \pi r^2 S \left(\frac{1-a}{2} \right) \left(1 - \frac{\sqrt{2hR + h^2}}{R + h} \right)$$

where:

a = earth's average albedo

h = sphere's altitude

r = sphere's radius

R = earth's radius

S = solar constant

Analysis for the earth reflected solar radiation, Q_A , is very involved because of the earth's shadowed hemisphere and the attendant geometric complexity.* The analytical development and curves for Q_A as a function of altitude and angular position are given in Reference 6.

In an effort to extend the utility of the flux program to a sphere approximation, the icosahedron was considered.

*If an unshadowed portion of the earth is "seen" by the sphere, $h < \frac{R}{\sin \theta}$ (1-sin θ) and $Q_A \approx 2\pi r^2 S a \left(1 - \frac{\sqrt{2hR+h^2}}{R+h} \right) \cos \theta_S$. Where θ_S is the angle between sun line and local vertical.

The icosahedron has been used as a sphere approximation in applications ranging from cartography to structural design. This regular solid has 20 faces which are congruent equilateral triangles. The circumscribing sphere contains all 12 vertices. Any of the six diameters through two corresponding opposite vertices contains the circumscribing sphere's center. Relative to any of these diameters the icosahedron can be considered as four contiguous right rectangular pyramids of five exposed faces each. The axes of the four pyramids are coincident with the diameter. Visualization of the two outside pyramids is easy since the apex vertices are the two diameter ends. The ten faces contained in the central zone between the two parallel five-sided bases of the end pyramids may be considered as portions of two truncated pyramids. The truncated portions of either of the two central 5-sided pyramids is the other pyramid. Of the 10 faces in the central zone, alternate faces belong to the two central polygons.

Orientation of the icosahedron in the orbit is accomplished by positioning a diameter coincident with the Z-axis (perpendicular to the orbital plane). Maintaining a base edge of either of the end pyramids perpendicular to the X-Z plane fixes the solid's circumferential position relative to the Z-axis. With this orbital orientation, the X-Z plane contains a normal of one face of each of the four considered pyramids. Figure 7 shows the solid's cross section in the X-Z plane with the four normals of interest. Input of these four normals and use of the flux program's spin capability allows the thermal fluxes on the solid's 20 sides to be simply determined

Detailed analysis not included here shows that the two necessary angles shown in Figure 7 between the normals and the Z-axis are

$$\theta = \cos^{-1} \left(\frac{1}{2 \cos 30 \tan 36} \right) = 37.4^\circ$$

$$\phi = \cos^{-1} \left[\frac{1}{2 \cos 30} \left(\frac{1}{\sin 36} - \frac{1}{\tan 36} \right) \right] = 79.2^\circ$$

With the Z-axis selected as the spin axis, μ_Z , δ_Z and δ_X are input as zero. The normals of the four faces whose rotation about the Z-axis will yield positions of the 20 faces are input as follows:

<u>Normal</u>	<u>β°</u>	<u>γ°</u>	<u>Number of Spin Increments</u>
N_1	0	37.4	6
N_2	0	79.2	6
N_3	0	217.4	6
N_4	0	259.2	6

The number of spin increments for each pyramid is input as six rather than five because of the program's inability to handle an odd number of increments.

Averaging the four pyramid's orbital average albedo flux gives an approximation whose accuracy is a function of angular position. For angles of 90° , 45° , and 0° between the solar vector and the local vertical radius vector, the respective percentage errors are +167%, -17%, and -29%. In a 230 NM circular orbit, the corresponding albedo fluxes from Reference 6 for the 90° and 0° limits are approximately 3.7 and 190 Btu/hr-ft². The maximum error incurred in using this approximation thus occurs at the lowest albedo flux with best accuracy expected at angles slightly greater than 45° . Increasing the number of spin increments from 6 to 24 yielded negligible differences.

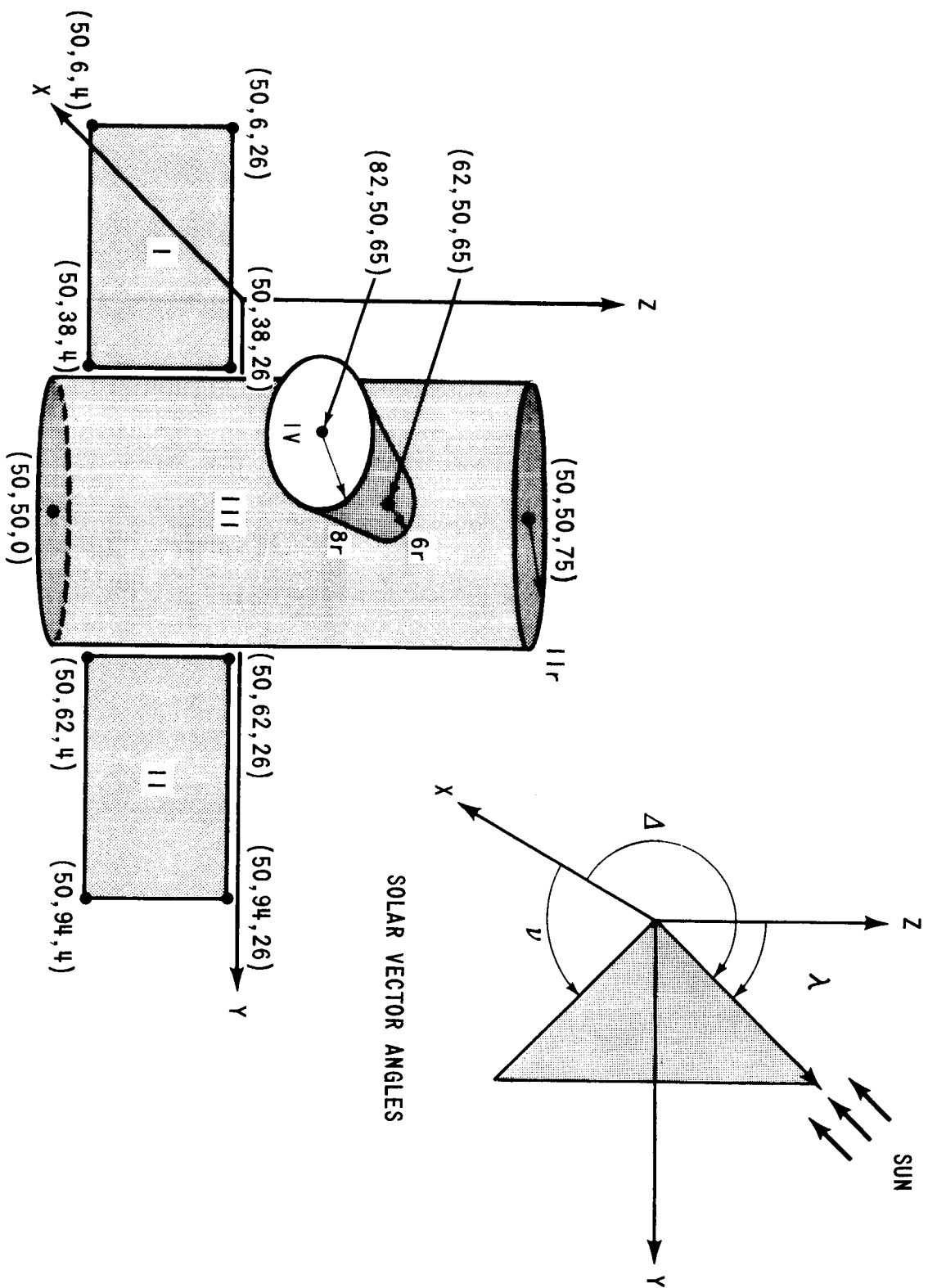


FIGURE 1 - SHADOWING PROGRAM SAMPLE PROBLEM, SPACECRAFT GEOMETRY

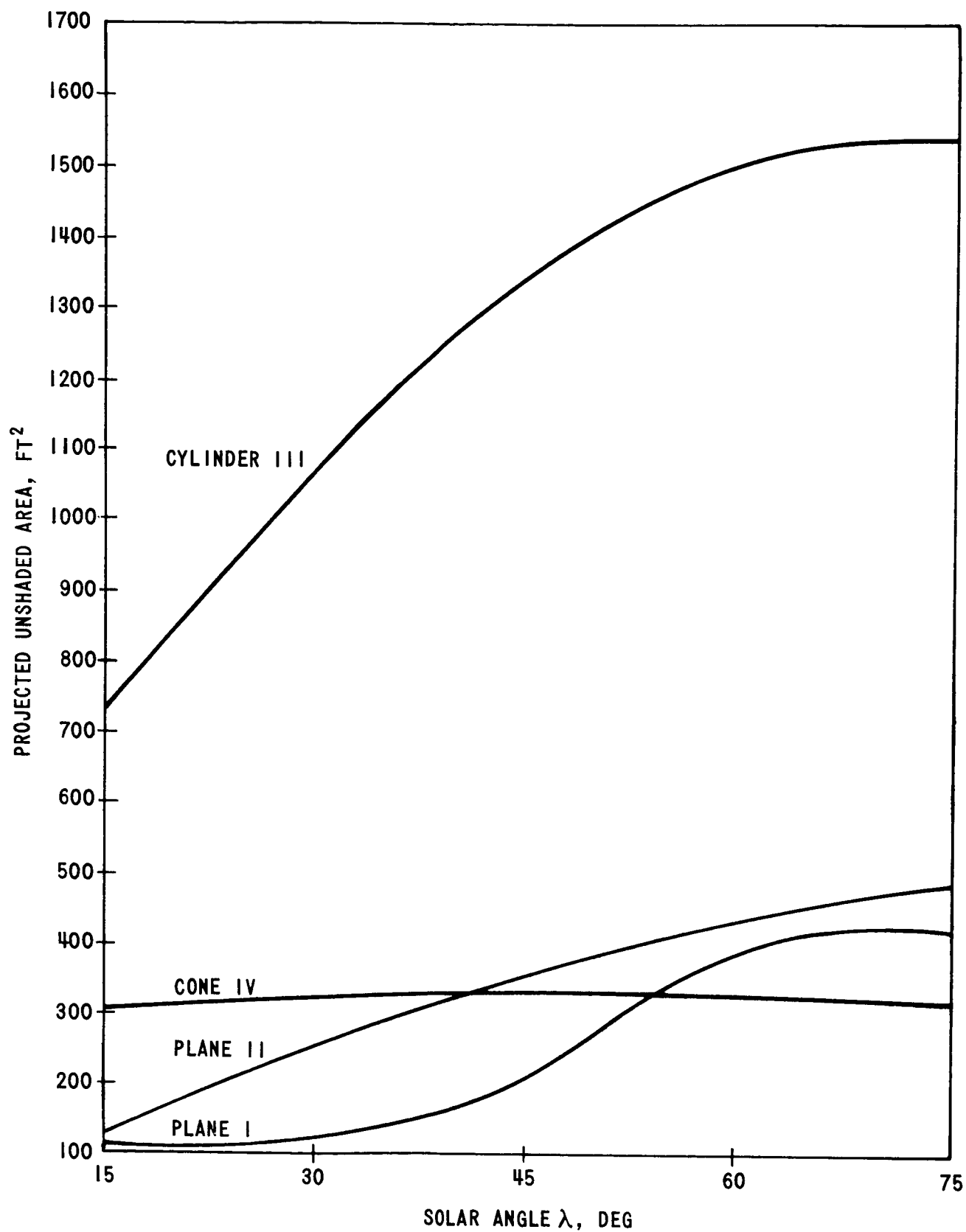


FIGURE 2 - SHADOWING PROGRAM SAMPLE PROBLEM UNSHADED PROJECTED AREA vs. SOLAR ANGLE λ FOR DIFFERENT SPACECRAFT COMPONENTS, SOLAR ANGLE $\nu = 45^\circ$

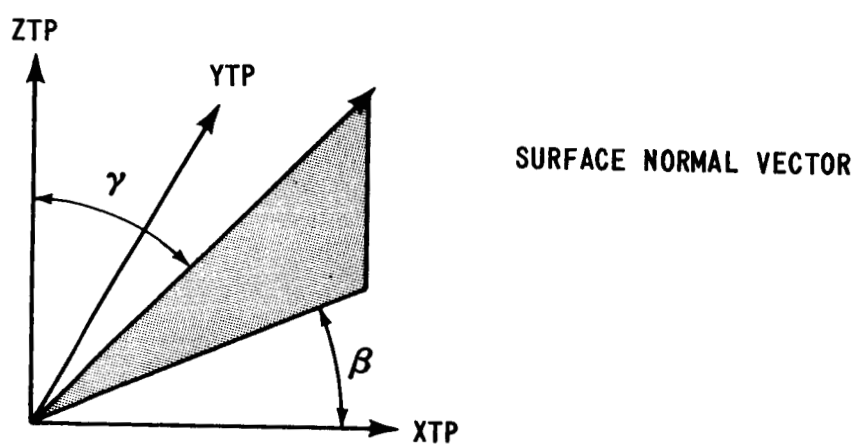
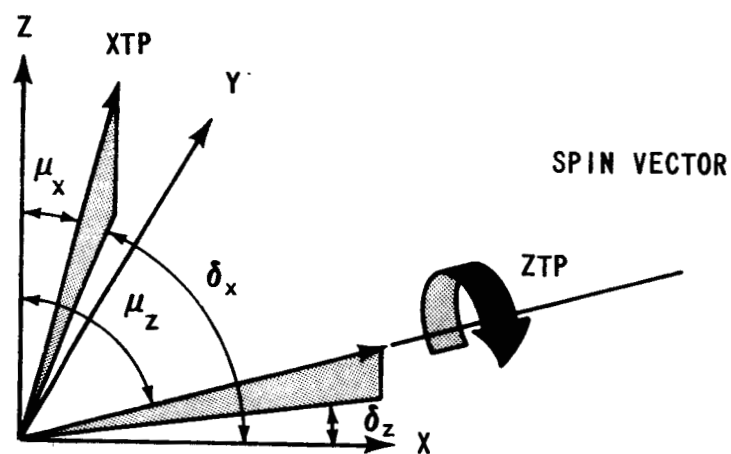
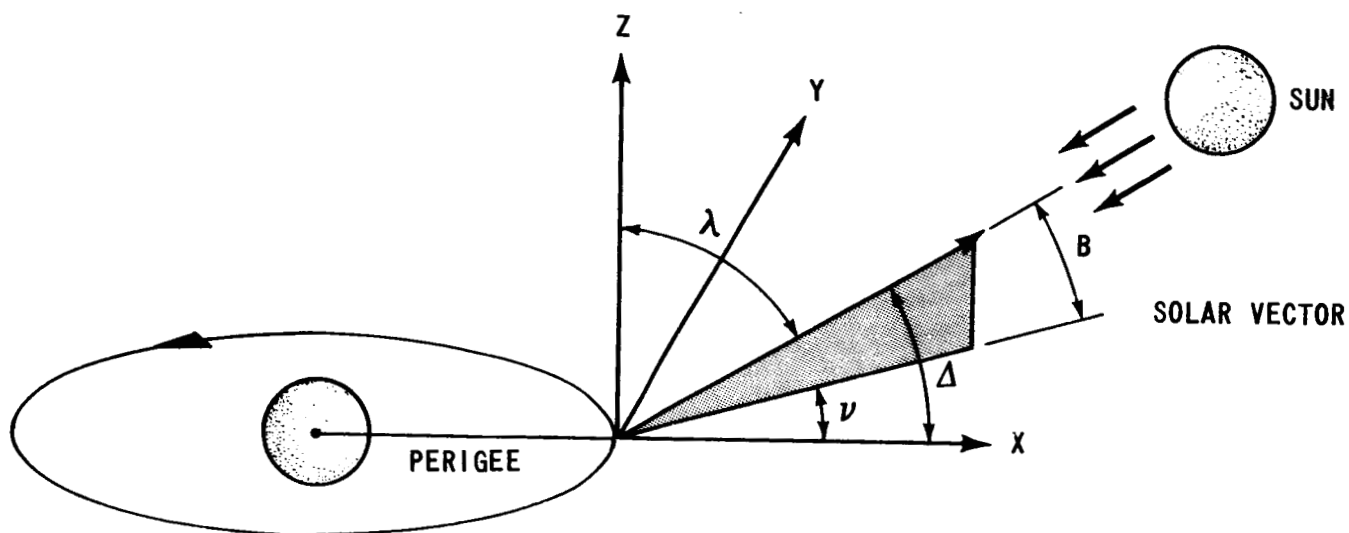


FIGURE 3 - FLUX PROGRAM COORDINATE SYSTEMS

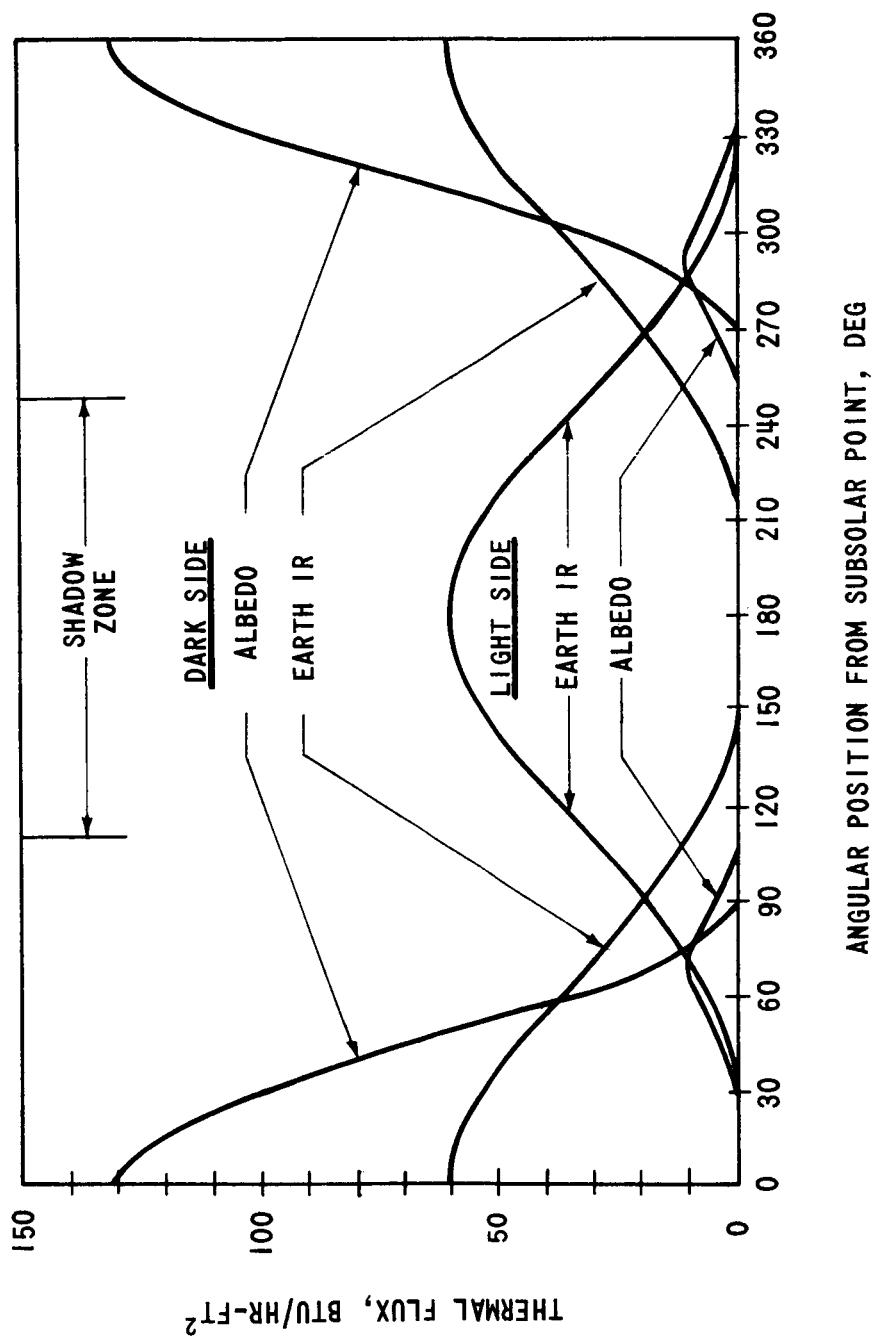


FIGURE 4 - THERMAL FLUX vs. ORBITAL POSITION FOR LIGHT & DARK SIDES OF UNIT AREA SURFACE NORMAL TO SUN LINE. 230 NM CIRCULAR EARTH ORBIT WITH SUN LINE IN ORBITAL PLANE, INERTIAL ORIENTATION

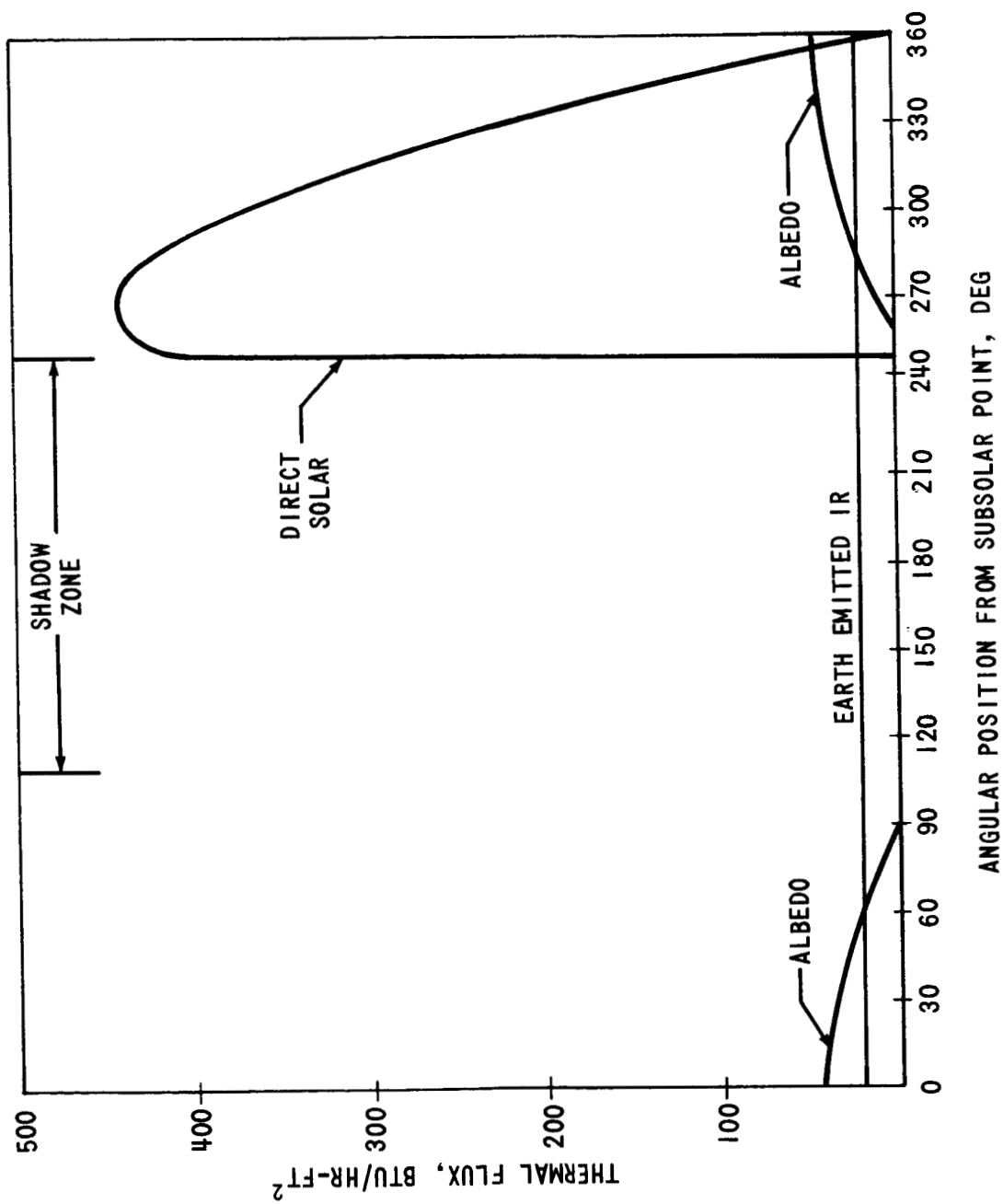
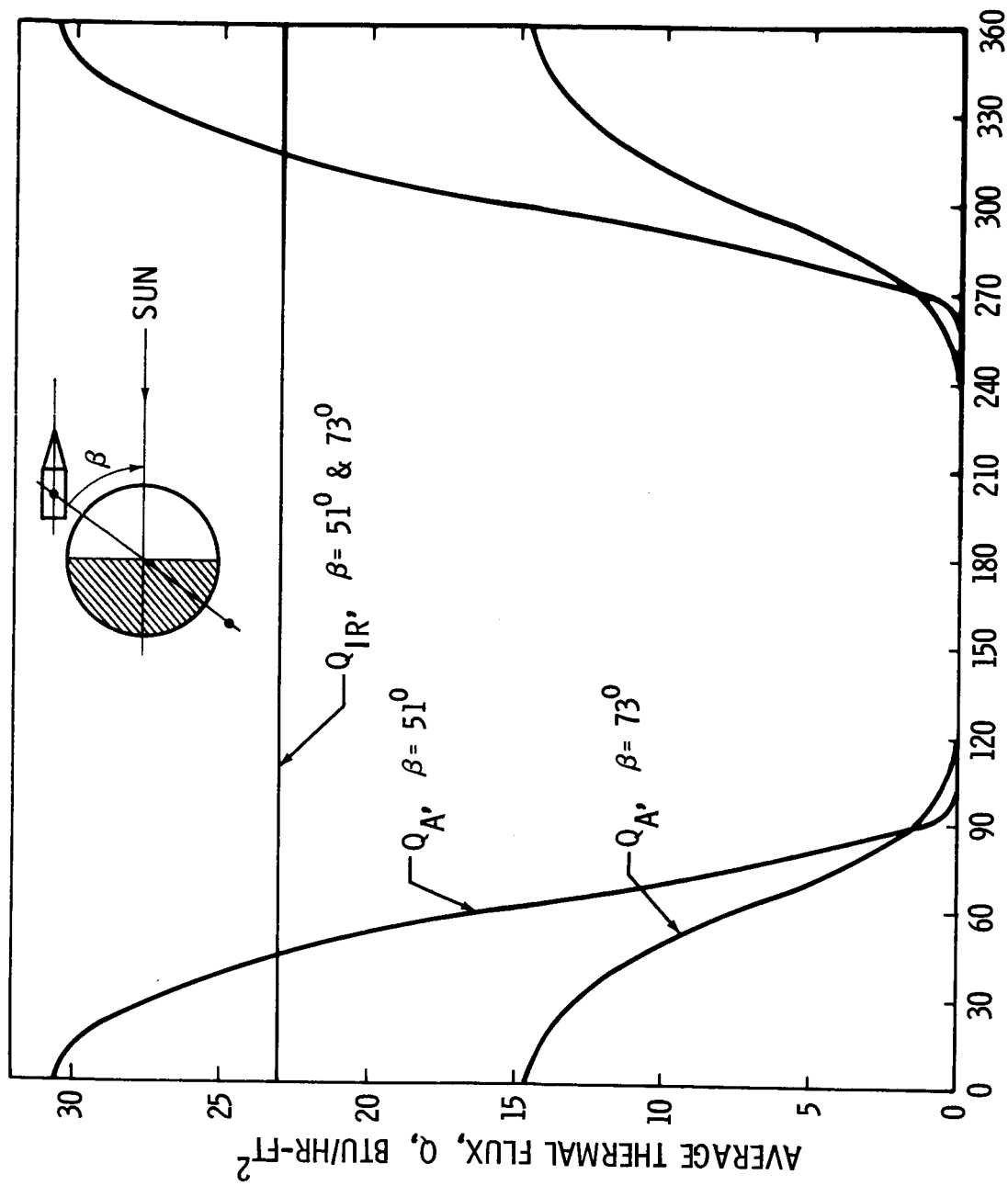


FIGURE 5 - THERMAL FLUX vs. ORBITAL POSITION FOR UNIT AREA NONSPINNING SURFACE IN GRAVITY GRADIENT ORIENTATION ($\beta = \gamma = 90^\circ$). 230 NM CIRCULAR ORBIT WITH SUN LINE IN ORBITAL PLANE



ANGULAR POSITION IN ORBIT MEASURED FROM SUBSOLAR POINT, DEG.

FIGURE 6 - AVERAGE ALBEDO (Q_A), & IR (Q_{IR}) THERMAL FLUX ON CSM LATERAL & END SURFACES, 230 NM CIRCULAR ORBIT, SUN POINTING INERTIAL ATTITUDE, NO SHADING BY SOLAR ARRAYS OR SPS NOZZLE

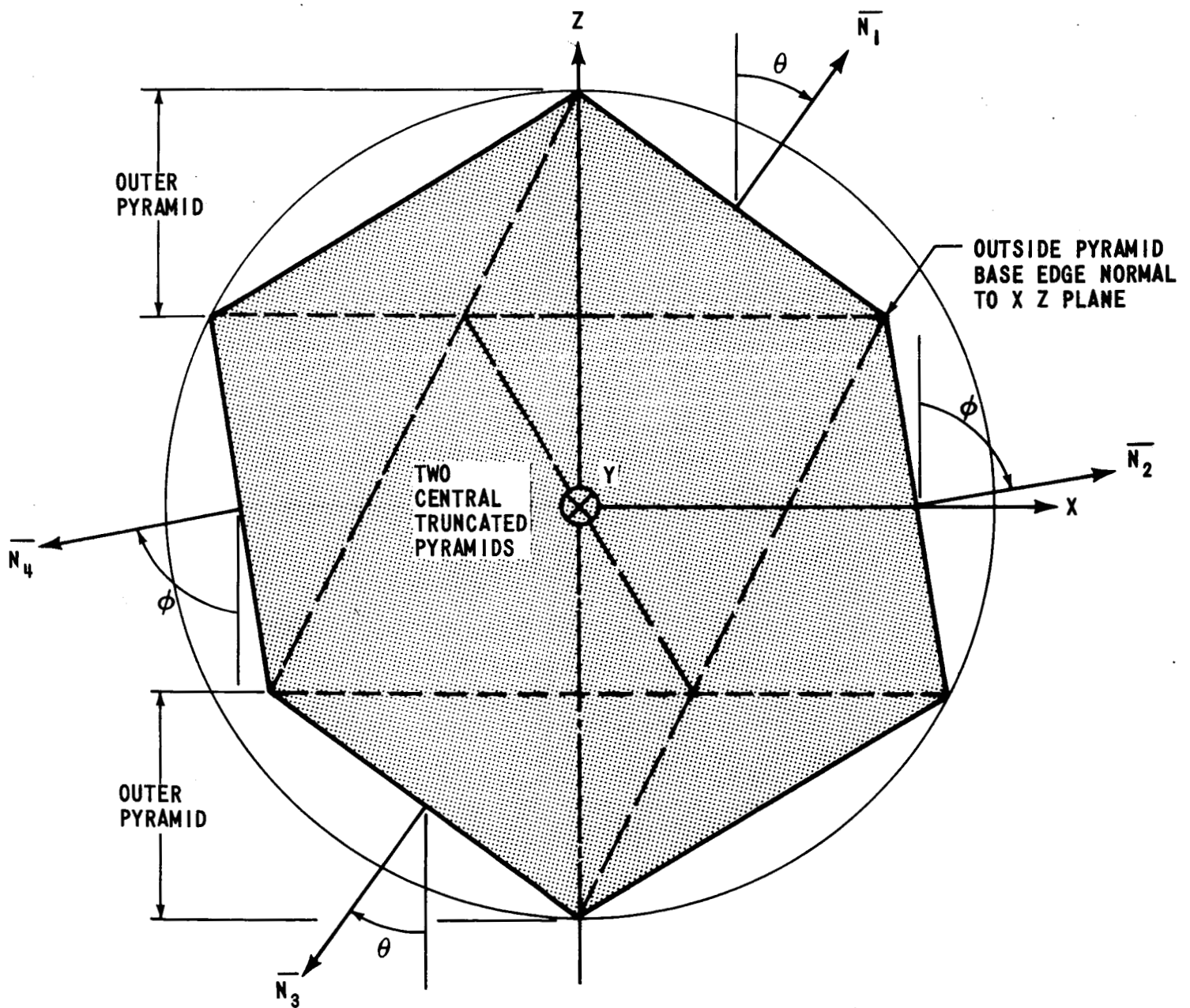


FIGURE 7 - CROSS SECTION OF ICOSAHEDRON SPHERE APPROXIMATION

BELLCOMM, INC.

REFERENCES

1. Skladany, J. T. and Rochkind, A. B., "Determination of Net Thermal Energy Incident on a Satellite", American Society of Mechanical Engineers, 67 HT-56.
2. Powers, E. I., "Thermal Radiation to a Flat Surface Rotating About an Arbitrary Axis in an Elliptical Earth Orbit", NASA Technical Note, TN D-2147, April 1964.
3. Orbital Flight Handbook, Volume I, NASA SP-33, Part 1, 1963, p III-4.
4. Hough, W. W., "The Effect of Launch Time on the Performance of a Solar Array/Battery Electrical Power System", Bellcomm Technical Memorandum, TM-67-1022-3, July 11, 1967, p 4.
5. Stevenson, J. A. and Grafton, J. C. "Radiation Heat Transfer Analysis for Space Vehicles, "Space and Information Systems Div., North American Aviation, Inc., SID 61-91, Dec 61, (ASD Repot 61-119, Contract AF 33 (616) - 7635), p. 80.
6. Cunningham, F. G., "Earth Reflected Solar Radiation Input to Spherical Satellites", NASA Technical Note TN-D1099, Oct. 1961.

BELLCOMM, INC.

Subject: Spacecraft Shadowing and Thermal
Flux Computer Programs with
Sample Problems

From: J. W. Powers

Distribution List

NASA Headquarters

Messrs. H. Cohen/MLR
P. E. Culbertson/MLA
J. H. Disher/MLD
J. A. Edwards/MLO
L. K. Fero/MLV
J. P. Field, Jr./MLP
T. A. Keegan/MA-2
H. T. Luskin/ML
C. P. Mook/RV-1
M. Savage/MLT

Bellcomm

Messrs. A. P. Boysen
D. A. Chisholm
D. R. Hagner
A. S. Haron
B. T. Howard
J. Z. Menard
T. L. Powers
I. M. Ross
J. A. Saxton
J. W. Timko
R. L. Wagner

GSFC

Messrs. J. Schach/713
J. T. Skladany/713

MSFC

Messrs. W. O. Randolph/R-P&VE-PTE
C. C. Wood/R-P&VE-PT

MSC

Messrs. R. Dotts/ES-5
R. E. Durkee/ES-5
R. L. Frost/KS

Division 101 Supervision
Departments 2015, 2034 Supervision
All Members Departments 1021, 1022, 1024
Department 1023
Central File
Library